

1 **Thermogravimetric Evaluation of Coal–Bagasse Blends for Co-Gasification**
2 **Applications: Effects of Operating Parameters on Thermal Conversion and**
3 **Kinetic Behavior**

4 Mahmood UI Hasan¹, Ahmad Hussain^{1,*}, Mehmood Ali²

5 ¹Department of Mechanical Engineering, DHA Suffa University, Karachi, Pakistan

6 ²Department of Environmental Engineering, NED University of Engineering and Technology,
7 Karachi, Pakistan

8 Emails: mahmood.hasan@dsu.edu.pk, ahmad.hussain@dsu.edu.pk (corresponding),
9 mehmood@neduet.edu.pk

10

11 **Abstract:**

12 This study evaluates the co-gasification suitability of coal–bagasse blends through
13 thermogravimetric analysis under non-isothermal conditions. Unlike studies that focus mainly on
14 single coal–biomass pairs, this work first screens multiple indigenous Pakistani coal samples and
15 agricultural residues and then evaluates the selected Chamalang coal–bagasse blends under
16 different operating conditions to identify a TGA-based optimum composition and operating
17 window. Indigenous coal and biomass samples were first characterized using proximate analysis,
18 ultimate analysis, and higher heating value determination, after which Chamalang coal and bagasse
19 were selected for blend preparation. Coal–bagasse blends of 94:6, 91:9, and 85:15 were examined
20 to determine the effects of operating conditions, including heating rate, feed composition, and
21 equivalence ratio, on thermal conversion behavior and kinetic characteristics. Thermogravimetric

22 experiments were conducted from ambient temperature to 950 °C. The thermograms showed clear
23 differences in the conversion behavior of coal, biomass, and blended fuels, confirming the strong
24 influence of volatile matter, fixed carbon, ash content, and inherent oxygen on reactivity. Among
25 the tested blends, the 91:9 coal–bagasse blend exhibited the most favorable overall performance.
26 The highest overall conversion was obtained at an equivalence ratio of 0.30 and a heating rate of
27 20 °C min⁻¹. Kinetic analysis further supported this result, with activation energies for the 91:9
28 blend reported as 26.75, 26.54, and 25.64 kJ mol⁻¹ at ER values of 0.25, 0.30, and 0.35,
29 respectively. These findings demonstrate the potential of optimized coal–bagasse blends for
30 efficient co-gasification system design.

31 **Keywords:** Coal–biomass blends; Coal–bagasse co-gasification; Thermogravimetric analysis;
32 Kinetic behavior; Biomass utilization; Thermal conversion

33 **1. Introduction**

34 Renewable energy has emerged as a key component of sustainable energy systems because it offers
35 a promising pathway to reduce dependence on fossil fuels, enhance energy security, and mitigate
36 environmental impacts (Ali et al., 2025; Ansari et al., 2026; Habib, 2026). The growing demand
37 for affordable and reliable energy, together with concerns over fossil fuel depletion and
38 environmental impact, has renewed interest in the thermochemical conversion of solid fuels
39 (Abedin et al., 2025; Ansari et al., 2026; Quan et al., 2026). Among the available options,
40 gasification offers an attractive route for converting low-grade solid feedstocks into useful gaseous
41 products while providing greater flexibility than direct combustion (Pribadi and Noble, 2026;
42 Ungureanu et al., 2025). Coal remains an important energy resource because of its large reserves
43 and established availability, but the direct use of low-rank coal is often limited by high moisture
44 or ash content and lower fuel quality (Balaram and Manikyamba, 2026; Lei et al., 2026; Nussipov
45 et al., 2026). In this context, gasification presents a more suitable pathway for utilizing such
46 resources efficiently (Inayat et al., 2025). At the same time, biomass has gained attention as a
47 renewable and widely distributed energy source that can partially substitute fossil fuels and
48 improve the sustainability of thermal conversion systems (Luo and Zhou, 2025).

49 Pakistan possesses substantial coal resources and also generates large amounts of agricultural
50 biomass residues, making coal–biomass co-gasification a practically relevant research direction
51 (Luo and Zhou, 2025). In particular, bagasse, rice husk, and corncob are available in appreciable
52 quantities and are already used to some extent as low-cost fuels in local industries (Jamil et al.,
53 2026; Mohlala et al., 2016). However, the direct use of biomass is often constrained by low bulk
54 density, variable moisture content, and lower energy density compared with coal (Bajwa et al.,
55 2018; TUMULURU and WRIGHT, 2010). Blending biomass with coal can therefore provide a

56 useful compromise by combining the higher volatile and oxygen content of biomass with the
57 higher fixed carbon and more stable feeding characteristics of coal (Bajwa et al., 2018;
58 TUMULURU and WRIGHT, 2010).

59 The performance of a fuel in gasification depends strongly on its physicochemical and thermal
60 characteristics. Properties such as volatile matter, fixed carbon, ash content, sulfur content, oxygen
61 content, heating value, and particle size influence ignition and devolatilization behavior, char
62 conversion, heat transfer, and the overall reactivity of the feedstock (Yadav et al., 2023). For
63 blended fuels, these effects become even more important because interactions between coal and
64 biomass components may alter the thermal response of the mixture (Si et al., 2024). For this reason,
65 careful characterization of candidate fuels is necessary before selecting a feedstock for gasification
66 or co-gasification applications (Awais et al., 2022).

67 Thermogravimetric analysis (TGA) is a useful technique for evaluating the thermal conversion
68 behavior of coal, biomass, and their blends because it provides continuous mass-loss information
69 as a function of temperature and time under controlled operating conditions (Yao et al., 2023;
70 Zhang et al., 2023). It is widely used to investigate decomposition behavior, thermal stability,
71 reactivity, and kinetic parameters of solid fuels (Gong and Yang, 2024). While many earlier studies
72 focused on pyrolysis and combustion, comparatively less attention has been given to blended fuels
73 under gasification or sub-stoichiometric conditions, particularly with respect to the influence of
74 operating parameters on both conversion behavior and kinetics (Koyunoğlu and Tolay, 2025;
75 Wang et al., 2025; Zein, 2026). Non-isothermal TGA is especially attractive for such analysis
76 because it enables comparison of thermal responses under practical heating programs and allows
77 estimation of kinetic parameters from conversion data (de Oliveira et al., 2022; Tarani and
78 Chrissafis, 2024).

79 In coal–biomass co-gasification, operating conditions play a decisive role in determining fuel
80 behavior. Parameters such as particle size, heating rate, blend composition, and equivalence ratio
81 affect devolatilization, char conversion, heat transfer, and the apparent kinetics of the process (Tian
82 et al., 2023). A systematic investigation of these variables is therefore essential for identifying
83 suitable feed blends and favorable operating windows for co-gasification applications (Adeoye et
84 al., 2026).

85 Unlike studies that focus mainly on single coal–biomass pairs, this work first screens multiple
86 indigenous Pakistani coal samples and agricultural residues and then evaluates the selected
87 Chamalang coal–bagasse blends under different operating conditions to identify a TGA-based
88 optimum composition and operating window. Therefore, the aim of this study is to evaluate the
89 suitability of selected indigenous coal, biomass, and coal–bagasse blends for co-gasification using
90 thermogravimetric analysis under non-isothermal, air-assisted conditions. The novelty of this work
91 lies in the integrated screening and optimization approach. First, four Pakistani coal samples and
92 three agricultural biomass residues were characterized through proximate analysis, ultimate
93 analysis, higher heating value determination, and thermogravimetric behavior. Second,
94 Chamalang sub-bituminous coal and sugarcane bagasse were selected based on their combined
95 fuel properties and thermal conversion performance. Third, coal–bagasse blends were investigated
96 at different blend ratios, heating rates, and equivalence ratios to determine their effects on
97 conversion behavior and apparent kinetic parameters. In this way, the study provides a feedstock-
98 specific and operating-condition-based assessment of indigenous coal–bagasse blends, offering a
99 clearer basis for selecting local fuels and identifying favorable operating windows for further co-
100 gasification development.

102 **2. Materials and Methods**

103 **2.1 Materials**

104 Four indigenous coal samples, namely Chamalang sub-bituminous coal (CHSB), Thar lignite
105 (THLig), Makarwal sub-bituminous coal (MAsub), and Salt Range sub-bituminous coal (SAsub),
106 were collected from coal-bearing regions of Balochistan, Sindh, and Punjab, Pakistan. Biomass
107 samples including bagasse, rice husk, and corncob were collected from local industrial sources
108 where these materials were being used as boiler fuel. All sample preparation and characterization
109 work was carried out at the Coal Research Centre, NFC Institute of Engineering and Technology,
110 Multan. Based on the initial fuel characterization, Chamalang coal and bagasse were selected for
111 blend preparation. Coal–bagasse blends were prepared in mass ratios of 94:6, 91:9, and 85:15 for
112 subsequent thermogravimetric evaluation under different operating conditions.

113 **2.2 Sample preparation and particle size classification**

114 The as-received coal samples were first crushed using a jaw crusher and then ground using a mortar
115 grinder. The ground coal was sieved into particle sizes of 710, 500, and 355 μm using a sieve
116 shaker. Bagasse was milled, dried, and subjected to sieve analysis to determine its average particle
117 size, which was found to be approximately 490 μm . On the basis of the preliminary evaluation,
118 coal of particle size 710 μm and bagasse of average particle size 490 μm were selected for blend
119 preparation and co-gasification analysis. The prepared samples were then used for proximate
120 analysis, ultimate analysis, heating value determination, and thermogravimetric testing.

121

122 **2.3 Physicochemical characterization**

123 ***2.3.1 Proximate analysis***

124 Proximate analysis of coal, biomass, and coal–bagasse blend samples was carried out using a
125 thermogravimetric analyzer (TGA-701). Approximately 80–110 mg of each sample was used for
126 analysis. All samples were prepared in triplicate, and the analyses were performed according to
127 ASTM D5142. The measured parameters included moisture content, volatile matter, fixed carbon,
128 and ash content. Average values of the three runs were reported and used to compare the fuel
129 characteristics of the investigated materials.

130 ***2.3.2 Ultimate analysis***

131 Ultimate analysis was performed using a LECO TruSpec CHNS analyzer to determine the
132 elemental composition of the coal and biomass samples. Carbon, hydrogen, and nitrogen were
133 measured using approximately 10 mg of sample, while sulfur determination was carried out
134 separately using larger sample quantities placed in ceramic crucibles. The CHNS analyzer was
135 operated with blank and standard runs between samples to ensure measurement reliability. Each
136 sample was analyzed in triplicate, and average values were reported on an as-received basis.
137 Oxygen content was determined by difference. The elemental composition data were later used to
138 interpret the thermal conversion behavior and kinetic characteristics of the fuels.

139 ***2.3.3 Higher heating value determination***

140 The higher heating value (HHV) of coal, biomass, and coal–bagasse blend samples was measured
141 using an automatic bomb calorimeter (LECO AC-500) according to ASTM D5865. Approximately

142 100 mg of each sample was used, and all measurements were performed in triplicate. During each
143 test, a measured quantity of sample was placed in the combustion vessel under pressurized
144 conditions and ignited. The temperature rise of the surrounding water was recorded by the
145 microprocessor-controlled calorimeter, and the corresponding HHV was determined. In addition
146 to the experimental measurements, the heating values of selected coal and biomass samples were
147 also estimated using Dulong's formula for comparison.

148 For proximate analysis, ultimate analysis, and higher heating value determination, repeated
149 measurements were performed and the average values were used for comparison of fuel properties.
150 However, the present study reports average values without standard deviation because the
151 complete replicate datasets were not available in a consistent form for all reported parameters.
152 Therefore, the reported values should be interpreted as representative average values for
153 comparative evaluation of the investigated fuels.

154 **2.4 Thermogravimetric analysis under co-gasification conditions**

155 Thermal conversion behavior of the prepared coal–bagasse blends was investigated using a
156 thermogravimetric analyzer operating in non-isothermal mode under controlled air atmosphere.
157 The blended samples were placed in ceramic crucibles and heated from ambient temperature to
158 950 °C. The effects of operating variables including feed composition, heating rate, and air flow
159 rate were studied systematically. Blend ratios of 85:15, 91:9, and 94:6 were tested. Heating rates
160 of 15, 20, and 40 °C min⁻¹ were employed, while air flow rates of 3.5 and 5.0 L min⁻¹ were used
161 to generate equivalence ratio (ER) values of 0.25, 0.30, and 0.35. Air was selected as the reaction
162 atmosphere in this study to represent air-assisted, sub-stoichiometric gasification conditions,
163 particularly for low-cost and decentralized gasification applications where air-blown operation is

164 commonly preferred because of its operational simplicity and lower oxidant cost. However, it is
165 recognized that industrial gasification systems may also employ steam, oxygen-enriched air,
166 oxygen–steam mixtures, or CO₂-containing atmospheres depending on the target syngas
167 composition and process design. Therefore, the present thermogravimetric results should be
168 interpreted primarily as a comparative evaluation of coal–bagasse blend behavior under air-
169 assisted conditions rather than as a complete representation of all industrial gasification
170 atmospheres. During each run, the initial sample mass and the corresponding mass loss with time
171 and temperature were recorded continuously throughout the thermal conversion process. It should
172 be emphasized that the thermogravimetric approach used in this study records only sample mass
173 loss as a function of temperature and time. Therefore, the results provide information on apparent
174 thermal conversion behavior, mass-loss stages, and kinetic response, but they do not directly
175 quantify gasification product quality. Parameters such as syngas composition, H₂/CO ratio, gas
176 heating value, tar concentration, carbon conversion to gas, and cold gas efficiency were not
177 measured in the present work. Consequently, the findings should be interpreted as a preliminary
178 thermogravimetric screening of coal–bagasse blend reactivity rather than a complete assessment
179 of gasification product performance. The operating conditions used for the thermogravimetric
180 experiments are summarized in **Table 1**.

181 **Table 1.** Operating conditions used for non-isothermal thermogravimetric analysis of coal–
182 bagasse blends from ambient temperature to 950 °C.

Run#	Sample	Sample weight (g)	Ramp rate (°C min ⁻¹)	Air flow (L min ⁻¹)	ER=Actual air/stoichiometric air
------	--------	----------------------	--------------------------------------	------------------------------------	--

1	91:9	2.092	40	3.5	0.30
2	85:15	3.5	20	5	0.25
	91:9	3.0			0.30
	94:6	2.5			0.35
3	85:15	2.5	20	3.5	0.25
	91:9	2.092			0.30
	94:6	1.80			0.35
4	91:9	2.092	15	3.5	0.30

183 Note: ER = equivalence ratio, defined as the ratio of actual air supplied to stoichiometric air requirement. Coal blend ratios are
 184 expressed on a mass basis. The temperature range for all TGA runs was from ambient temperature to 950 °C.

185 The thermogravimetric experiments were used to compare the relative conversion behavior of the
 186 selected coal–bagasse blends under controlled operating conditions. The TGA results are presented
 187 as representative conversion profiles for each condition. Since complete repeated TGA datasets
 188 were not available for every blend ratio, heating rate, and equivalence ratio, error bars and standard
 189 deviations were not included for the conversion curves. This limitation should be considered when
 190 interpreting small differences between operating conditions; therefore, the main conclusions were
 191 drawn from consistent overall trends in conversion behavior and kinetic response rather than from
 192 minor point-to-point variations.

193 2.5 Conversion calculation

194 The extent of thermal conversion of the coal–bagasse blends during thermogravimetric analysis
 195 was determined from the mass-loss data using the following expression:

$$\alpha = \frac{W_i - W_t}{W_i - W_\infty} \quad (1)$$

196 where W_i is the initial sample mass, W_t is the sample mass at time t , and W_∞ is the final residual
197 mass after completion of the thermal conversion process. This expression was used to compare the
198 conversion behavior of the blended fuels under different operating conditions.

199 **2.6 Kinetic modeling**

200 *2.6.1 Kinetic assumptions*

201 The kinetic analysis of thermal conversion was carried out using thermogravimetric mass-loss
202 data. For the purpose of kinetic modeling, the following assumptions were adopted: the reaction
203 was considered to be kinetically controlled, the thermal decomposition process was approximated
204 by a first-order reaction model, and the influence of heat-transfer limitations was neglected
205 because of the relatively small particle size of the samples. These assumptions were used to
206 simplify the estimation of the apparent kinetic parameters from the non-isothermal
207 thermogravimetric data. It should be noted that the first-order Arrhenius-based model used in this
208 study provides apparent kinetic parameters for comparative purposes. Solid-fuel co-gasification is
209 a complex process involving overlapping devolatilization, char conversion, mineral-catalyzed
210 reactions, and possible heat- and mass-transfer effects. Therefore, the assumption of a single first-
211 order reaction does not fully represent the complete reaction mechanism. The activation energies
212 reported in this work should be interpreted as model-dependent apparent values rather than
213 intrinsic kinetic constants.

214 *2.6.2 Arrhenius-based non-isothermal kinetic model*

215 Using the conversion term defined in Eq. (1), the general rate equation for solid-state thermal
216 conversion can be written as

$$\frac{d\alpha}{dt} = k(T)f(\alpha) \quad (2)$$

217 where $k(T)$ is the temperature-dependent rate constant and $f(\alpha)$ is the reaction model function.

218 According to the Arrhenius relation,

$$k(T) = A \exp\left(\frac{-E_a}{RT}\right) \quad (3)$$

219 Substituting Eq. (3) into Eq. (2) gives

$$\frac{d\alpha}{dt} = A \exp\left(\frac{-E_a}{RT}\right) (1 - \alpha)^n \quad (4)$$

220 where A is the pre-exponential or frequency factor, E_a is the activation energy, R is the universal
221 gas constant, T is the absolute temperature, and n is the reaction order.

222 Under a constant heating rate condition,

$$\beta = \frac{dT}{dt} \quad (5)$$

223 where β is the heating rate. Substituting Eq. (5) into Eq. (4) gives

$$\frac{d\alpha}{dT} = \frac{A}{\beta} \exp\left(\frac{-E_a}{RT}\right) (1 - \alpha)^n \quad (6)$$

224 Rearranging and integrating Eq. (6) yields

$$\int_0^\alpha \frac{d\alpha}{(1-\alpha)^n} = \frac{A}{\beta} \int_{T_0}^T \exp\left(\frac{-E_a}{RT}\right) dT \quad (7)$$

225 For $n \neq 1$, the integral form becomes

$$\frac{1 - (1-\alpha)^{1-n}}{1-n} = \frac{A}{\beta} \int_{T_0}^T \exp\left(\frac{-E_a}{RT}\right) dT \quad (8)$$

226 and for the first-order model ($n = 1$),

$$-\ln(1-\alpha) = \frac{A}{\beta} \int_{T_0}^T \exp\left(\frac{-E_a}{RT}\right) dT \quad (9)$$

227 Since the temperature integral has no exact analytical solution, an asymptotic approximation was
228 used. Accordingly, the linearized form for $n \neq 1$ can be expressed as

$$\ln\left[\frac{1 - (1-\alpha)^{1-n}}{(1-n)T^2}\right] = \ln\left(\frac{AR}{\beta E_a}\right) - \frac{E_a}{RT} \quad (10)$$

229 For the first-order reaction model used in this study, the final linearized form becomes

$$\ln\left[\frac{-\ln(1-\alpha)}{T^2}\right] = \ln\left(\frac{AR}{\beta E_a}\right) - \frac{E_a}{RT} \quad (11)$$

230 In the present work, the reaction order was assumed to be unity for all operating conditions in
231 order to simplify the analysis and to enable direct comparison among coal, biomass, and coal–
232 bagasse blend samples.

233 **2.6.3 Determination of kinetic parameters**

234 For the first-order model, the kinetic parameters were determined from the linear relationship
235 given in Eq. (11) by plotting

$$\ln \left[\frac{-\ln(1 - \alpha)}{T^2} \right] \text{ versus } \frac{1}{T} \quad (12)$$

236 The slope of the straight line is equal to $-E_a/R$, while the intercept is equal to $\ln (AR/(\beta E_a))$.
237 Therefore, the activation energy (E_a) and frequency factor (A) were calculated from the slope and
238 intercept of the fitted line. The values of conversion α and absolute temperature T obtained from
239 the thermogravimetric curves were used in the analysis, and the best acceptable kinetic parameters
240 were selected on the basis of the linear correlation coefficient.

241 **3. Results and Discussion**

242 **3.1 Physicochemical characterization of coal and biomass samples**

243 The physicochemical properties of the selected coal and biomass samples were evaluated through
244 proximate analysis, ultimate analysis, and higher heating value determination in order to identify
245 suitable feedstocks for co-gasification. The results show clear differences between the indigenous
246 coal samples and biomass materials in terms of volatile matter, fixed carbon, ash content, elemental
247 composition, and calorific value. These variations are important because they directly influence
248 fuel reactivity, devolatilization behavior, char conversion, and the overall suitability of the
249 feedstock for thermochemical conversion. These fuel-property results support the later selection
250 of Chamalang coal and bagasse for blend preparation.

251 The proximate analysis and experimentally measured higher heating values of the coal and
 252 biomass samples are presented in **Table 2**. Among the biomass samples, bagasse exhibited the
 253 highest volatile matter and the lowest ash content, indicating favorable reactivity and cleaner
 254 thermal conversion behavior. Corncob also showed appreciable volatile matter and fixed carbon,
 255 whereas rice husk had comparatively lower volatile matter and higher ash content, which may limit
 256 its suitability for gasification applications. Among the coal samples, Chamalang sub-bituminous
 257 coal showed the most balanced fuel characteristics, with moderate volatile matter, high fixed
 258 carbon, low ash content, and a favorable heating value. In contrast, Salt Range coal contained very
 259 high ash, which may adversely affect reactivity and increase the possibility of ash-related
 260 operational problems during thermal conversion. Thar lignite exhibited a lower heating value,
 261 while Makarwal coal, although having relatively high volatile matter and heating value, contained
 262 more ash than Chamalang coal. These results indicate that Chamalang coal is the most suitable
 263 coal sample among those investigated for subsequent co-gasification studies.

264 **Table 2.** Proximate analysis and measured higher heating values of indigenous coal and biomass
 265 samples, with selected literature comparisons.

Characteristics	Volatile (%)	Fixed Carbon (%)	Ash (%)	HHV MJ kg ⁻¹	References
Bagasse	81.33	12.28	5.35	17.88	This study
Bagasse	83.2	10.06	6.9	17.06	(Vamvuka et al., 2003)
Bagasse	79.90	18.00	2.20	(db)18.	(Rodrigues et al., 2011)

Corncob	60.04	29.85	6.61	16.41	This study
Corncob	83.5	15.5	1.0	17.9	(Zakaria et al., 2010)
Rice husk	48.21	31.86	10.31	14.29	This study
Rice husk	68.0	17	15	16.2	(Youssef et al., 2009)
Rice husk	62.95	13.49	18.15	14.80	(Youssef et al., 2009)
Low Rank (ar)CH _{SB}	39.8	51	8.3	22.20	This study
Low Rank (ar) MA _{Sub}	46.95	28.56	14.42	28.56	This study
PRB Coal	40.83	50.34	8.83	26.60	(Wang et al., 2012)
Low Rank (ar) SA _{Sub}	35.03	30.48	33.34	19.82	This study
Low rank (ar) TH _{Lig}	22.93	39.25	4.95	13.25	This Study
Lignite (ar)TH	23.96	40.14	14.28	15.53	(Sarwar et al., 2012)
Thailand Low rank Coal	36.68	19.24	25.70	---	(Rodjeen et al., 2006)
Low rank Malaysian Coal	43.0	53.3	3.7	25.2	(Youssef et al., 2009)
Medium Rank coal	25.1	68.5	6.4	32.0	(Youssef et al., 2009)

Low rank	45.4	45.3	9.3	28.7	(Youssef et al., 2009)
----------	------	------	-----	------	---------------------------

266 Note: CHSB = Chamalang sub-bituminous coal; MA_{sub} = Makarwal sub-bituminous coal; SA_{sub} = Salt Range sub-bituminous
267 coal; THLig = Thar lignite; ar = as-received basis; db = dry basis; HHV = higher heating value. Biomass abbreviations: BG =
268 bagasse, CC = corncob, RH = rice husk.

269 The ultimate analysis results and heating values estimated using Dulong's formula are summarized
270 in **Table 3**. The biomass samples contained higher oxygen and lower carbon contents than the coal
271 samples, which is consistent with their generally lower heating values but higher expected
272 reactivity. Bagasse showed a favorable combination of carbon, hydrogen, and oxygen contents,
273 supporting its selection as the biomass component for blend preparation. Among the coal samples,
274 Chamalang and Makarwal coals showed comparatively higher carbon contents and higher
275 calculated heating values than Thar lignite and Salt Range coal. Thar lignite contained lower
276 carbon and higher oxygen, while Salt Range coal exhibited an unfavorable sulfur and ash profile.
277 These elemental trends complement the proximate analysis results and further support the selection
278 of Chamalang coal and bagasse as suitable fuels for co-gasification.

279 **Table 3.** Ultimate analysis and higher heating values estimated using Dulong's formula for coal
280 and biomass samples, with selected literature comparisons.

Samples	N (%)	C (%)	H (%)	S (%)	O (%) (By diff)	HHV BY Dulong's Formula (Mj/Kg)	Ref
THLig (ar)	0.98	31.90	7.17	0.99	54.01	11.41	Present study

Lignite (daf)	3.88	58.0	11.18	0.68	25.16	14.17	(Senneca et al., 1999)
. (ar) CH _{SB}	1.40 9	59.08	5.60	2.79	22.82	24.22	Present study
Sub- bit coal (daf)	1.95	72.98	7.01	0.71	17.00	20.50	(Senneca et al., 1999)
Wyoming Sub- bit coal (daf)	1.07	75.68	4.43	0.45	18.37	27.11	(Fryda et al., 2006)
Colombia bituminous coal (dry)	1.58	75.69	5.29	1.57	7.91	30.634	(Preciado et al., 2012)
Coal	1.89	75.8	4.40	1.22	16.7	-	(Puig-Arnavat et al., 2010)
(ar)SA _{Sub}	1.57	43.64	3.93	13.12	4.4	20.79	Present study
(ar)MA _{Sub}	1.56	71.79	6.04	0.77	5.43	31.99	Present study

Ba	1.41	43.07	6.6	0.16	43.41	16.22	Present study
Bagasse	0.16	49.86	6.02	0.17	40.19	18.53	(NREL, 1995)
Bagasse	0.60	44.60	5.80	0.10	44.50	18.00	(Rodrigues et al., 2011)
Ch	1.37	42.85	5.4	0.15	45.54	14.03	Present study
Corncob	0.64	45.04	5.79	-	48.53	--	(Rodjeen et al., 2006)
Rh	1.39	36.45	5.43	4.82	41.59	13.07	Present study
Rice Husk	0.14	37.85	5.20	0.61	27.65	-	(Youssef et al., 2009)

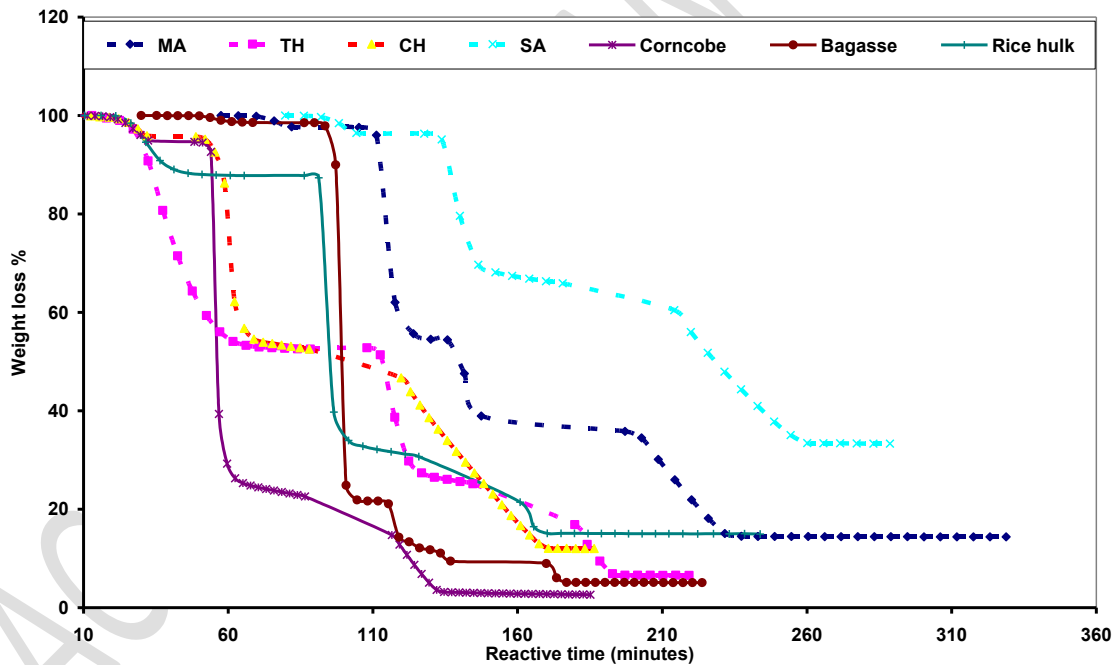
281 Note: N = nitrogen; C = carbon; H = hydrogen; S = sulfur; O = oxygen calculated by difference; HHV = higher heating value
282 estimated using Dulong's formula. THLig = Thar lignite; CHS_b = Chamalang sub-bituminous coal; SASub = Salt Range sub-
283 bituminous coal; MASub = Makarwal sub-bituminous coal; Ba = bagasse; Cc = corncob; Rh = rice husk; ar = as-received basis;
284 daf = dry ash-free basis.

285 Overall, the combined results of proximate analysis, ultimate analysis, and heating value
286 determination indicate that Chamalang coal and bagasse are the most appropriate coal and biomass
287 samples, respectively, for preparing blended fuels. Chamalang coal was preferred because of its
288 relatively high fixed carbon, low ash content, and acceptable heating value, whereas bagasse was
289 selected because of its high volatile matter, low ash content, and favorable elemental composition.

290 These properties make the selected pair suitable for investigating the thermal conversion behavior
291 of coal–bagasse blends under different co-gasification operating conditions.

292 3.2 Thermogravimetric behavior of individual coal and biomass samples

293 The thermogravimetric behavior of the individual coal and biomass samples was evaluated under
294 non-isothermal heating conditions in order to compare their conversion characteristics and identify
295 the most suitable feedstocks for subsequent co-gasification studies. As shown in **Figure 1**, the
296 thermograms of both coal and biomass samples can be broadly divided into three main stages:
297 initial moisture release, devolatilization, and subsequent conversion of the residual char.



298
299 **Figure 1.** Thermogravimetric conversion behavior of individual coal and biomass samples under
300 non-isothermal heating conditions from ambient temperature to 950 °C.

301 In the first stage, the initial mass loss corresponds primarily to moisture removal from the fuel
302 matrix. This stage was more pronounced for fuels with higher inherent moisture, particularly Thar
303 lignite, which is consistent with its lower thermal conversion efficiency during later stages. The
304 second stage represented devolatilization, where the release of volatile compounds occurred more
305 rapidly in biomass than in coal. The biomass thermograms were steeper in this region, indicating
306 faster conversion and greater reactivity. This behavior is consistent with the higher volatile matter
307 and oxygenated organic fractions of biomass, which promote decomposition at relatively lower
308 temperatures. The stronger devolatilization behavior of biomass can be attributed to its higher
309 content of thermally reactive constituents, and the biomass samples showed higher overall
310 conversion than coal under the same conditions.

311 Among the biomass samples, bagasse and corncob exhibited the highest overall thermal
312 conversion, while rice husk showed comparatively lower conversion. The overall conversion
313 values are reported as approximately 98% for bagasse, 96% for corncob, and 84% for rice husk.
314 The comparatively lower conversion of rice husk can be linked to its higher ash content, whereas
315 the superior behavior of bagasse reflects its high volatile matter and lower ash fraction. These
316 results are consistent with the fuel-property trends already discussed in Section 3.1 and provide
317 further support for the selection of bagasse as the biomass component for blend preparation.

318 The coal samples showed slower and less extensive conversion than the biomass samples,
319 particularly in the devolatilization region. Among the coals, Chamalang sub-bituminous coal
320 exhibited the most favorable thermal behavior. Although Thar lignite is inherently more reactive
321 than higher-rank coals, its elevated moisture content reduced its effective conversion performance
322 under the tested conditions. Salt Range coal showed the poorest suitability because of its very high

323 ash content, which can suppress reactivity and may also promote ash-related operational problems
324 during co-gasification. Makarwal coal exhibited comparatively high volatile matter and heating
325 value, but its ash content remained higher than that of Chamalang coal.

326 The third stage of the thermograms corresponded to the conversion of the residual char at higher
327 temperatures. This region is important because it reflects the ability of the remaining carbonaceous
328 material to continue reacting after the devolatilization phase. In general, the coal samples retained
329 more residual mass than the biomass samples, which is consistent with their higher fixed-carbon
330 content and lower overall conversion under the same non-isothermal conditions. Therefore, the
331 thermogravimetric analysis of the individual fuels confirms that bagasse and Chamalang coal are
332 the most suitable biomass and coal feedstocks, respectively, for investigating coal–bagasse blends
333 under co-gasification conditions.

334 **3.3 Physicochemical characterization of coal–bagasse blends**

335 Based on the physicochemical characterization and thermogravimetric behavior of the individual
336 fuels, Chamalang coal and bagasse were selected for the preparation of blended feedstocks for co-
337 gasification analysis. Coal–bagasse blends were prepared at mass ratios of 94:6, 91:9, and 85:15
338 in order to examine the effect of biomass addition on the fuel properties of the parent coal. The
339 visual appearance of the prepared blends is shown in **Figure 2**, while their proximate analysis and
340 higher heating value data are summarized in **Table 4**.



85:15

91:9

94:6

341 **Figure 2.** Physical appearance of coal–bagasse blends prepared at selected mass ratios

342 The progressive addition of bagasse to Chamalang coal altered the physicochemical characteristics
343 of the blended fuels in a systematic manner. As shown in **Table 4**, increasing the biomass fraction
344 increased the volatile matter content of the blends while reducing the fixed carbon content relative
345 to the parent coal. This behavior is expected because bagasse is more volatile and more oxygen-
346 rich than coal. The moisture content also showed a slight increase with biomass addition, reflecting
347 the more hygroscopic nature of bagasse. In contrast, the ash content remained within a
348 comparatively moderate range, indicating that the selected biomass did not introduce the high ash
349 burden typically associated with less favorable agricultural residues such as rice husk. These trends
350 are important because higher volatile matter can enhance ignition and devolatilization, whereas
351 excessive ash can hinder reactivity and reduce conversion efficiency during thermochemical
352 processing.

353 **Table 4.** Proximate analysis and measured higher heating values of Chamalang coal and coal–
354 bagasse blends prepared at different mass ratios.

Sample	Moisture	Volatile matter	Fixed Carbon	Ash	Calorific value.
Coal:Bagasse	(%)	(%)	(%)	(%)	MJ/kg
94:06	0.917	42.2918	48.6768	8.123	21.9408
91:09	0.920	43.5377	47.5152	8.0345	21.8112
85:15	0.928	46.0295	45.192	7.8575	21.552

355 Note: Coal blend ratios are expressed on a mass basis. HHV values are reported in MJ kg⁻¹. Moisture, volatile matter, fixed
356 carbon, and ash contents are reported as weight percentages.

357 The higher heating values of the blends remained reasonably close to that of the parent coal, despite
358 the addition of biomass. This indicates that partial substitution of coal by bagasse did not cause a
359 severe reduction in energy content within the investigated blending range. Among the tested
360 mixtures, the 91:9 blend provided the most favorable balance between volatile matter enhancement
361 and acceptable calorific value. Thus, the blend-property data provide an important preliminary
362 indication that moderate bagasse addition can improve the reactive characteristics of the fuel
363 without significantly compromising its energy value.

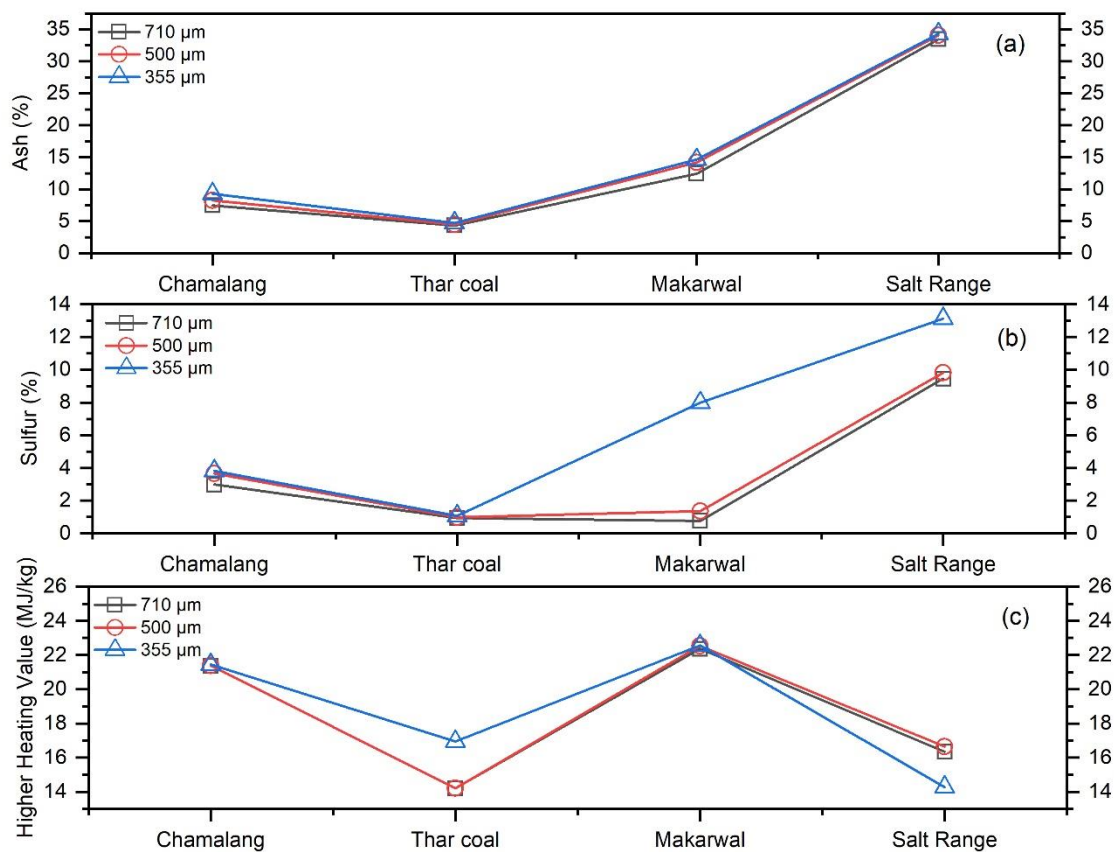
364 The observed property changes in the blended fuels are consistent with the individual
365 characteristics of Chamalang coal and bagasse discussed in Sections 3.1 and 3.2. Chamalang coal
366 contributed relatively high fixed carbon and stable fuel value, while bagasse contributed higher
367 volatile matter and improved reactivity potential. Therefore, blending these two fuels offers a
368 practical route for producing a composite feedstock with more favorable characteristics for co-
369 gasification than the raw coal alone. On this basis, the prepared coal–bagasse blends were selected
370 for detailed evaluation of the effects of operating conditions on thermal conversion behavior in the
371 following section.

372 **3.4 Effect of operating parameters on conversion behavior**

373 *3.4.1 Effect of particle size*

374 Particle size is an important fuel parameter because it affects surface area, heat transfer, release of
375 volatile matter, and the accessibility of the solid matrix to reacting gases. As the coal particle size
376 decreased from 710 to 355 μm , the release of sulfur and ash changed noticeably, and the heating
377 value of most coal samples improved. The decreasing particle size increased the release of ash and
378 sulfur and generally improved the heating value for all coals except Salt Range coal. This behavior
379 was attributed to enhanced reactivity resulting from the larger surface area and higher porosity of
380 smaller particles.

381 The improvement associated with smaller particles is also relevant from a process standpoint.
382 Reduced particle size promotes faster heating and more efficient removal of volatile products from
383 the particle surface, which can improve the thermal conversion performance of the fuel. In
384 addition, smaller particles are more compatible with fluidized-bed operation because they help
385 maintain more stable fluidization and reduce the tendency for excessive inert ash accumulation.
386 However, the response was not identical for all coal types. Salt Range coal showed a reduction in
387 heating value after size reduction, which attributes to the release of inorganic combustible sulfur
388 with the ash fraction. Therefore, although particle size reduction generally improved fuel behavior,
389 the extent of the benefit depended on the mineral and sulfur characteristics of the individual coal.
390 Overall, the particle-size analysis supports the use of suitably reduced coal size for co-gasification
391 applications. Since smaller particles provide faster heat transfer and greater reactivity, they are
392 expected to favor improved gasification performance. On this basis, the selected coal size was
393 considered appropriate for subsequent blending and thermogravimetric conversion experiments.

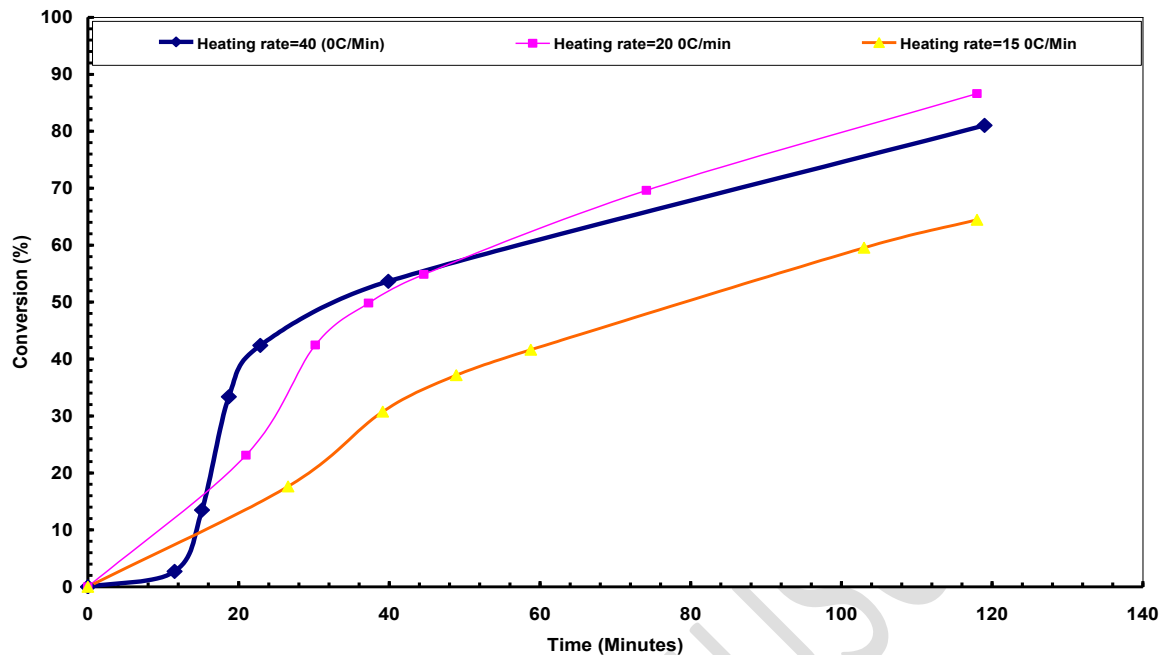


394

395 **Figure 3.** Effect of coal particle size on fuel properties of the investigated coal samples: (a) ash
 396 content, (b) sulfur content, and (c) higher heating value.

397 3.4.2 Effect of heating rate

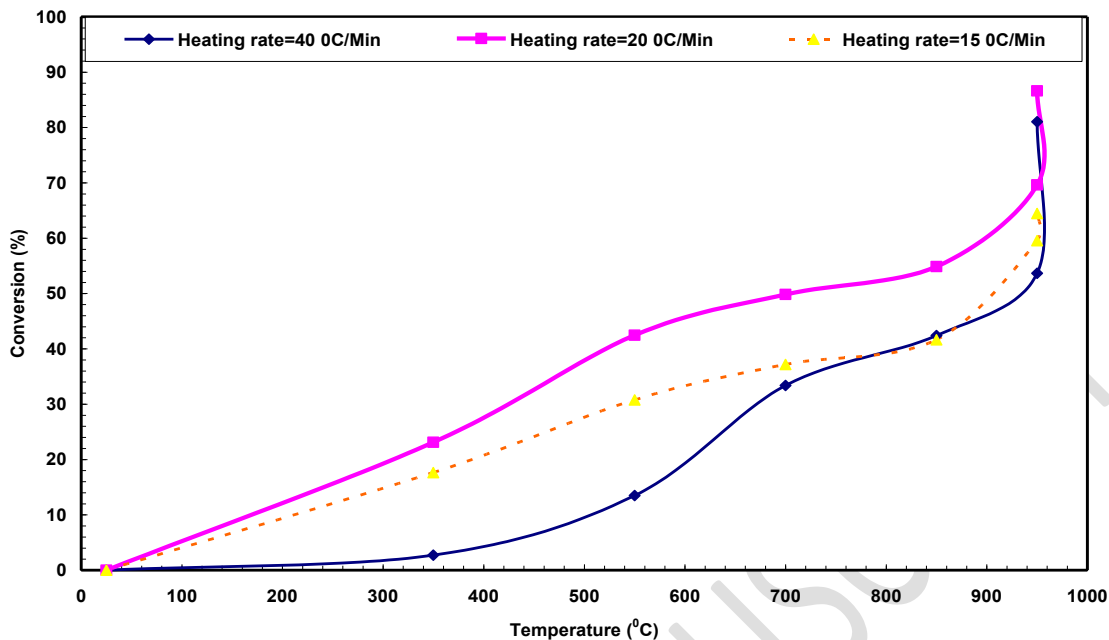
398 The effect of heating rate on thermal conversion was investigated using the 91:9 coal–bagasse
 399 blend under otherwise fixed conditions. The thermograms showed that changing the heating rate
 400 altered both the position and the shape of the conversion curves. Increasing the heating rate from
 401 15 to 40 °C min⁻¹ caused a shift in the thermograms, with the curves requiring different times to
 402 reach the main devolatilization region. The reported times to attain approximately 700 °C were
 403 48.88, 37.25, and 18.72 min for heating rates of 15, 20, and 40 °C min⁻¹, respectively.



404

405 **Figure 4.** Effect of heating rate on the conversion behavior of the 91:9 coal–bagasse blend under
 406 air-assisted conditions at ER = 0.30.

407 It is to be noted that within the lower temperature range, up to about 700 °C, the highest conversion
 408 rate was observed at 20 °C min⁻¹, with a value of 49.82%, whereas corresponding values at 40 and
 409 15 °C min⁻¹ were 37.49% and 37.16%, respectively. At higher temperatures, between 700 and 950
 410 °C, the conversion behavior changed because the remaining char underwent further
 411 thermochemical reactions. In this region, the 40 °C min⁻¹ condition showed a stronger
 412 instantaneous conversion contribution, but the highest overall conversion was still obtained at 20
 413 °C min⁻¹. These results indicate that an intermediate heating rate provided the best balance between
 414 devolatilization and subsequent char conversion.



415

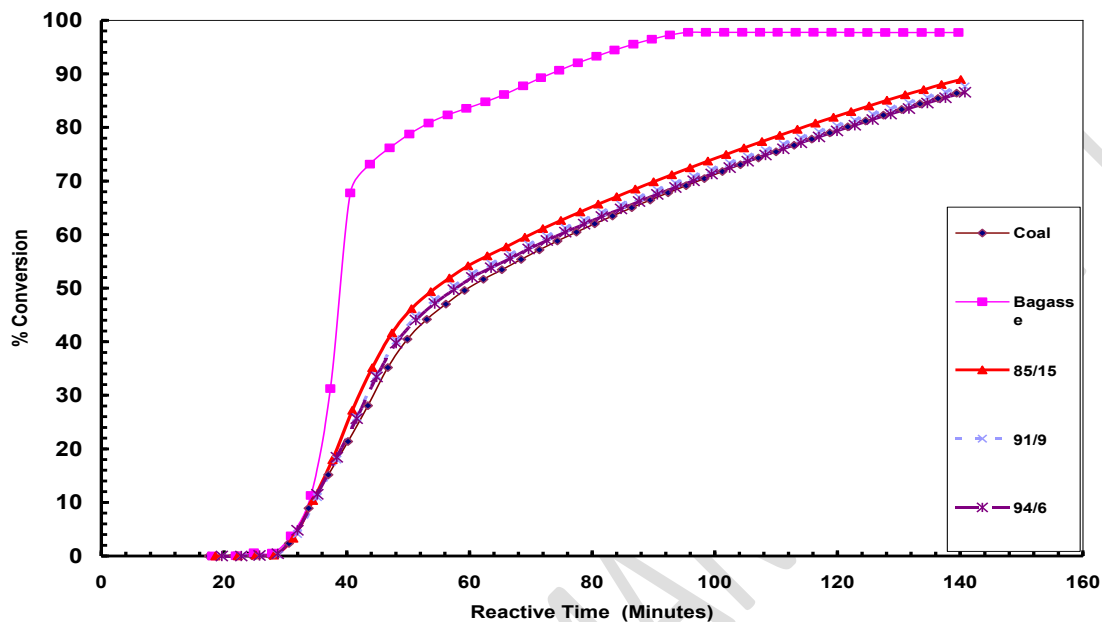
416 **Figure 5.** Thermogravimetric curves of the 91:9 coal–bagasse blend at heating rates of 15, 20,
 417 and 40 °C min⁻¹ under air-assisted conditions.

418 This behavior can be explained by the competing effects of heat supply and thermal uniformity.
 419 At very low heating rate, the process becomes slower and the conversion remains limited. At very
 420 high heating rate, heat is supplied rapidly, but local non-uniformity and incomplete utilization of
 421 the volatile-release stage may reduce the overall effectiveness of the process. Therefore, the results
 422 suggest that 20 °C min⁻¹ is the most suitable heating rate among the tested values for coal–bagasse
 423 co-gasification under the present thermogravimetric conditions.

424 **3.4.3 Effect of feed composition**

425 The feed composition had a clear influence on the thermal conversion behavior of the coal–bagasse
 426 blends. Increasing the fraction of bagasse increased the oxygen availability and volatile matter
 427 content of the feedstock, while lowering the fixed carbon and slightly reducing the heating value,

428 as already seen in Table 4. The higher oxygen content of biomass can reduce the effective oxidant
429 demand of the mixture and promote the partial oxidation reactions involved in gasification.



430
431 **Figure 6.** Effect of coal:bagasse blend ratio on thermal conversion behavior at a heating rate of
432 $20\text{ }^{\circ}\text{C min}^{-1}$ and $\text{ER} = 0.30$.

433 As shown by the conversion curves, increasing the biomass fraction enhanced the reactivity of the
434 blend. With increasing biomass content from 94:6 to 91:9 and 85:15, the reactivity of the feedstock
435 increased due to the higher volatile fraction, greater inherent oxygen availability, and lower ash
436 content. At the same time, heating value decreased with increasing biomass fraction, which means
437 that reactivity enhancement must be balanced against the decline in fuel energy density. This is an
438 important practical observation because excessive biomass addition may improve conversion but
439 reduce the calorific strength and bulk handling quality of the feed.

440 It should be noted that the improved conversion behavior observed after bagasse addition
441 represents the apparent co-conversion performance of the blended fuels under the investigated
442 thermogravimetric conditions. In this study, a formal quantitative synergy index was not calculated
443 because rigorous synergistic or antagonistic interaction analysis requires complete conversion
444 profiles of the individual coal and biomass samples under exactly the same operating conditions
445 as each corresponding blend. Therefore, the observed enhancement in reactivity should be
446 interpreted as an indication of improved blend performance rather than direct quantitative proof of
447 synergistic interaction. Future work should include theoretical additive conversion analysis, in
448 which the experimental blend conversion is compared with the weighted conversion of individual
449 coal and bagasse, to quantify the degree of synergy or antagonism during co-gasification.

450 Therefore, feed composition must be optimized rather than simply maximizing the biomass
451 fraction. The results suggest that moderate addition of bagasse improves conversion behavior
452 without causing an excessive penalty in heating value. This later supports the selection of the 91:9
453 blend as the most suitable composition for further operating and kinetic analysis.

454 The enhanced conversion behavior of the coal–bagasse blends can also be interpreted from a
455 micro-mechanistic perspective. During heating, bagasse decomposes earlier than coal because of
456 its higher volatile matter and oxygenated organic structure. The rapid release of volatiles from
457 biomass can contribute to the formation of additional pores and channels within the blended char
458 matrix, thereby improving heat transfer and increasing the accessibility of reacting gases to the
459 remaining carbonaceous material. Similar effects of biomass addition on volatile release, char
460 structure, and coal–biomass interaction have been reported in previous studies on coal–biomass
461 thermal conversion (Vamvuka et al., 2003; Wang et al., 2012; Tian et al., 2023).

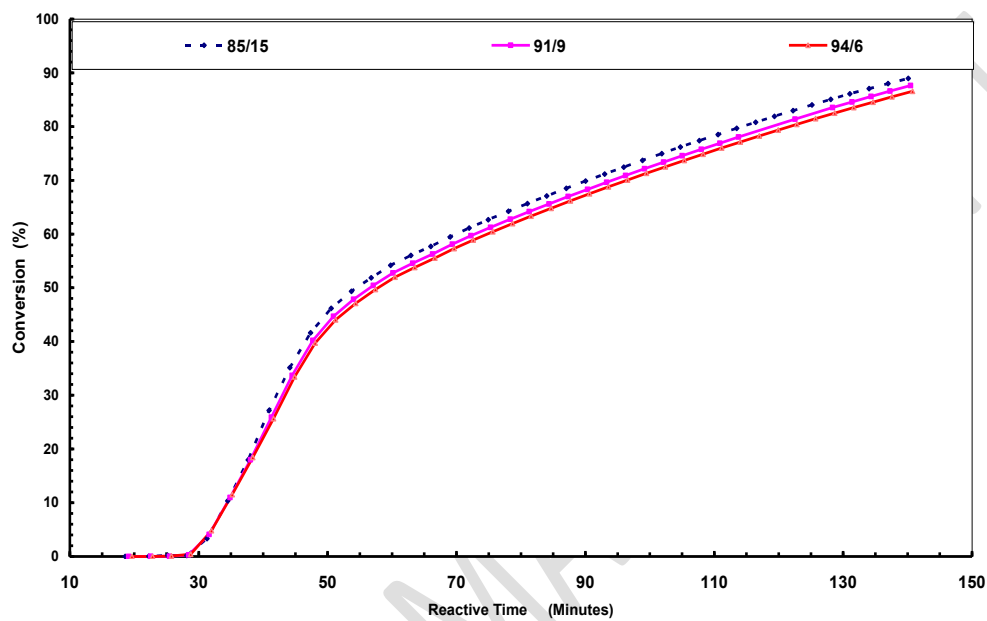
462 In addition, biomass-derived ash may contain mineral species that can influence char conversion
463 reactions. Alkali and alkaline earth metals present in biomass ash are commonly considered to
464 promote carbon conversion by increasing active reaction sites and facilitating oxygen transfer
465 during thermochemical reactions (Puig-Arnavat et al., 2010; Yadav et al., 2023). The oxygen-rich
466 structure of bagasse may also promote the formation of oxygenated volatiles and surface functional
467 groups during decomposition, which can improve the local reactivity of the coal–biomass matrix.
468 Therefore, the improved performance of the coal–bagasse blends may be associated not only with
469 bulk fuel properties such as volatile matter, ash content, and heating value, but also with pore
470 evolution, catalytic mineral effects, and oxygen-assisted reaction pathways. However, these
471 mechanisms are inferred from the observed thermogravimetric behavior and literature evidence;
472 direct confirmation would require additional char characterization.

473 ***3.4.4 Effect of equivalence ratio***

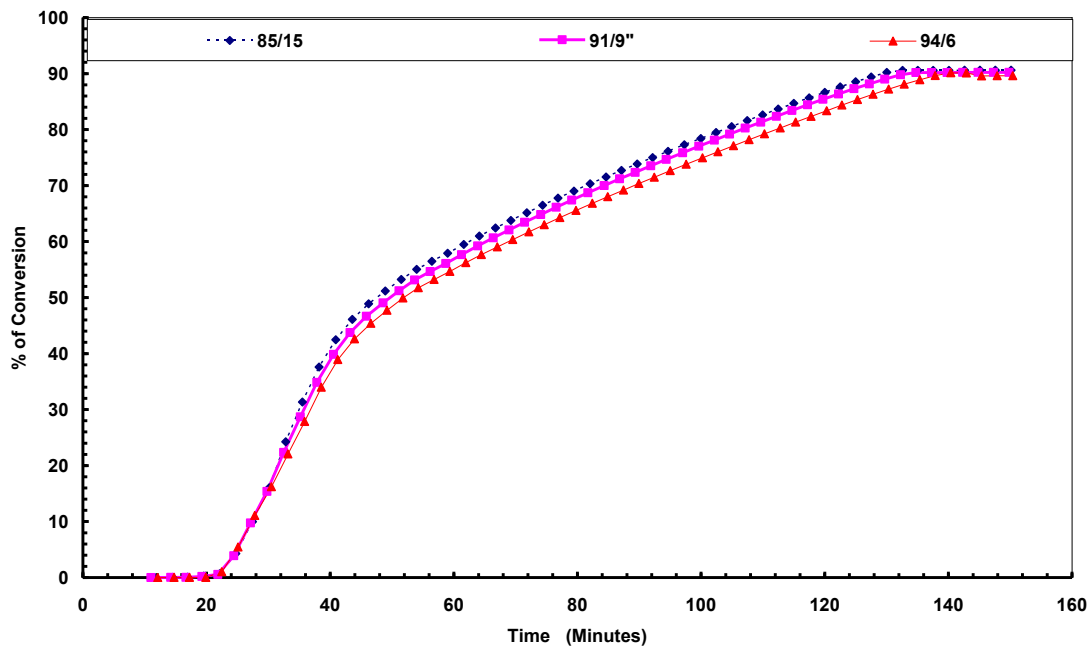
474 Equivalence ratio is one of the most important operating variables in gasification because it
475 controls the amount of oxidant available for combustion and partial oxidation reactions. In the
476 present study, ER values of 0.25, 0.30, and 0.35 were evaluated for the coal–bagasse blends while
477 keeping the other operating conditions fixed. The increase in air supply increased the ER and
478 improved the conversion process. This is reasonable because a higher oxidant supply promotes
479 greater heat release and enhances the conversion of devolatilized and charred material.

480 Figures 7 to 9 compare the conversion behavior of the three blends at ER values of 0.25, 0.30, and
481 0.35. The conversion increased as ER increased, which is consistent with the expected role of
482 oxidant supply in raising gasification intensity. However, ER = 0.30 was identified as the best
483 overall condition, rather than ER = 0.35, when conversion performance and kinetic suitability were

484 considered together. This shows that although higher ER promotes conversion, there is still an
485 optimum range beyond which the process may shift away from the desired balance between
486 gasification and partial combustion.

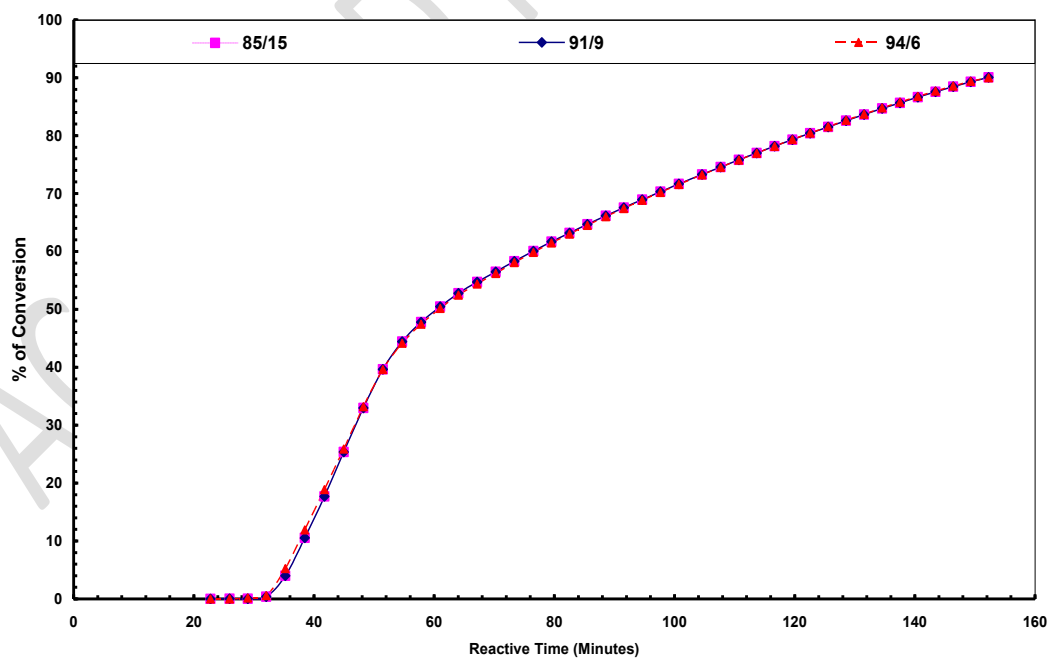


487
488 **Figure 7.** Thermal conversion of coal–bagasse blends at ER = 0.25 and a heating rate of 20 °C
489 min⁻¹.



490

491 **Figure 8.** Thermal conversion of coal–bagasse blends at ER = 0.30 and a heating rate of 20 °C
 492 min⁻¹.



493

494 **Figure 9.** Thermal conversion of coal–bagasse blends at ER = 0.35 and a heating rate of 20 °C
495 min⁻¹.

496 Thus, the ER study demonstrates that oxidant supply strongly affects thermal conversion and must
497 be carefully controlled for efficient co-gasification performance. Within the present operating
498 window, an ER of 0.30 provided the most favorable balance and was therefore selected as the
499 optimum condition for the 91:9 coal–bagasse blend. The use of air as the gasifying atmosphere
500 also means that the observed effect of equivalence ratio reflects the combined influence of oxygen
501 availability and nitrogen dilution under air-assisted conditions. In steam or oxygen-enriched
502 gasification, the reaction pathway and product-gas composition may differ because steam
503 promotes water–gas and water–gas shift reactions, while oxygen enrichment reduces nitrogen
504 dilution and can increase the heating value of the produced gas. Therefore, the optimum ER
505 identified in the present study is specific to the investigated air-assisted thermogravimetric
506 conditions. Further studies under steam, oxygen-enriched air, and mixed gasifying atmospheres
507 are required to extend these findings to broader industrial gasification systems.

508 **3.5 Kinetic results and discussion**

509 The kinetic analysis was carried out to further interpret the thermogravimetric conversion behavior
510 of the investigated coal, biomass, and coal–bagasse blends under different operating conditions.
511 Using the first-order Arrhenius-based non-isothermal model described in Section 2.6, the apparent
512 activation energy and frequency factor were estimated from the thermogravimetric data. The
513 resulting kinetic parameters provide an additional basis for comparing the thermal reactivity of the
514 different fuels and for identifying the most favorable operating conditions for co-gasification.

515 The kinetic results should be interpreted with consideration of the limitations of the adopted model.
516 The first-order Arrhenius approach was selected to provide a simple and consistent basis for
517 comparing the apparent kinetic behavior of the investigated fuels and blends. However, coal–
518 biomass co-conversion usually involves multiple overlapping reaction stages, including moisture
519 release, devolatilization, volatile–char interaction, and high-temperature char conversion. Model-
520 free isoconversional methods, such as Flynn–Wall–Ozawa, Kissinger–Akahira–Sunose, and
521 Starink methods, can provide more detailed information by evaluating activation energy at
522 different conversion levels without assuming a fixed reaction order. Such approaches are
523 particularly useful for complex solid-state reactions and have been recommended for improving
524 the reliability of kinetic interpretation in thermogravimetric studies (de Oliveira et al., 2022; Tarani
525 and Chrissafis, 2024). Since complete multi-heating-rate datasets were not available for all blend
526 compositions and equivalence ratios in the present work, the kinetic analysis was limited to
527 apparent first-order parameters. Therefore, the activation-energy values reported here are used
528 mainly for relative comparison among fuels, blend ratios, and operating conditions.

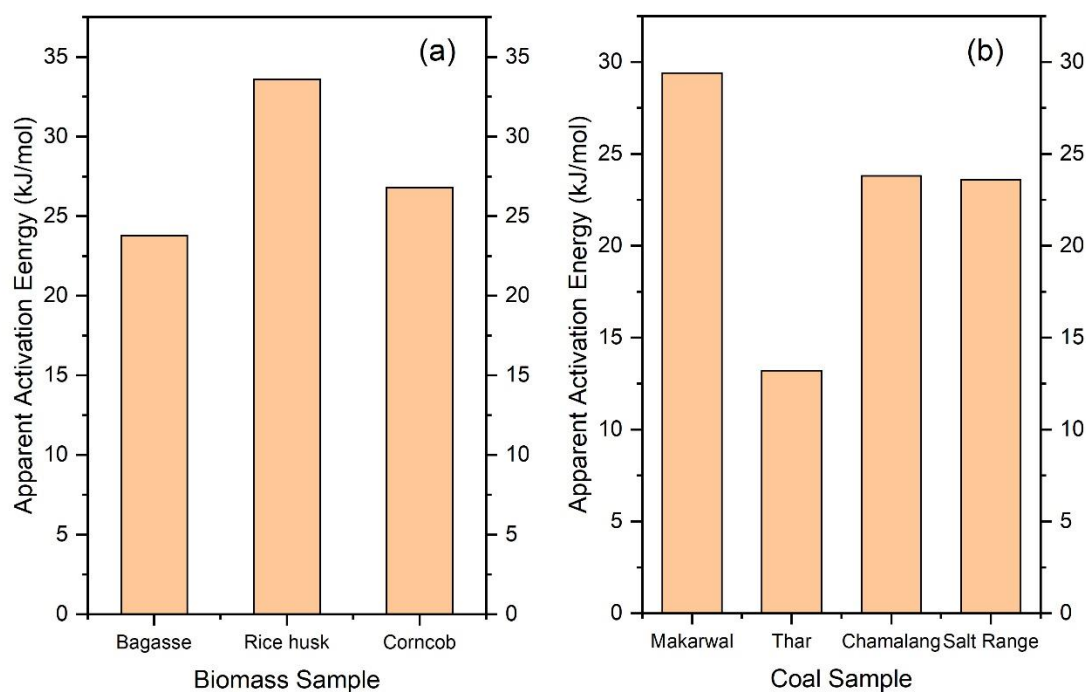
529 The lower apparent activation energy observed for bagasse and selected coal–bagasse blends may
530 be associated with microstructural and catalytic effects during thermal conversion. Biomass
531 decomposition generally occurs at lower temperatures than coal decomposition, leading to earlier
532 volatile release and the possible development of a more porous char structure. This can improve
533 gas diffusion and increase the accessibility of reactive sites during subsequent char conversion.
534 Previous studies have also reported that coal–biomass blending can modify volatile-release
535 behavior, char structure, and apparent kinetic response during thermochemical conversion
536 (Zakaria et al., 2010; Wang et al., 2012; Tian et al., 2023).

537 The presence of biomass-derived mineral matter may also contribute to the improved kinetic
538 behavior of the blends. Mineral species such as potassium, calcium, magnesium, and sodium,
539 which are often present in biomass ash, can act as catalytic species during char conversion and
540 may reduce the apparent energy barrier of the reaction (Puig-Arnavat et al., 2010; Yadav et al.,
541 2023). Furthermore, the higher oxygen content of bagasse can promote oxygen-containing
542 intermediates and surface functional groups, which may enhance the reactivity of the blended fuel.
543 These mechanisms are consistent with the improved apparent conversion and lower activation-
544 energy trends observed for the coal–bagasse blends. However, because the present study did not
545 include SEM, BET, XRD, FTIR, or ash elemental analysis of the residual chars, the proposed
546 mechanisms should be regarded as explanatory interpretations rather than direct experimental
547 confirmation.

548 The activation energies obtained for the biomass samples are presented in **Figure 10**. Among the
549 tested biomasses, bagasse showed the lowest activation energy, followed by corncob and rice husk.
550 This indicates that bagasse required the least energy input to initiate and sustain thermal
551 conversion, which is consistent with its higher volatile matter content, lower ash fraction, and
552 better overall thermogravimetric performance observed in the earlier sections. Rice husk showed
553 the highest activation energy among the biomass samples, which can be attributed to its
554 comparatively high ash content and less favorable conversion behavior. These results provide
555 kinetic support for selecting bagasse as the biomass component in the coal–biomass blends.

556 The activation energies of the investigated coal samples are shown in **Figure 10**. Chamalang sub-
557 bituminous coal exhibited the most favorable kinetic behavior among the coals, with lower
558 activation energy than the less suitable alternatives. Salt Range coal showed comparatively less

559 favorable behavior, which is consistent with its high ash content and inferior physicochemical
560 characteristics. Thar lignite and Makarwal coal showed intermediate behavior. The kinetic results
561 therefore complement the proximate, ultimate, and thermogravimetric analyses and further justify
562 the selection of Chamalang coal for preparation of the coal–bagasse blends.



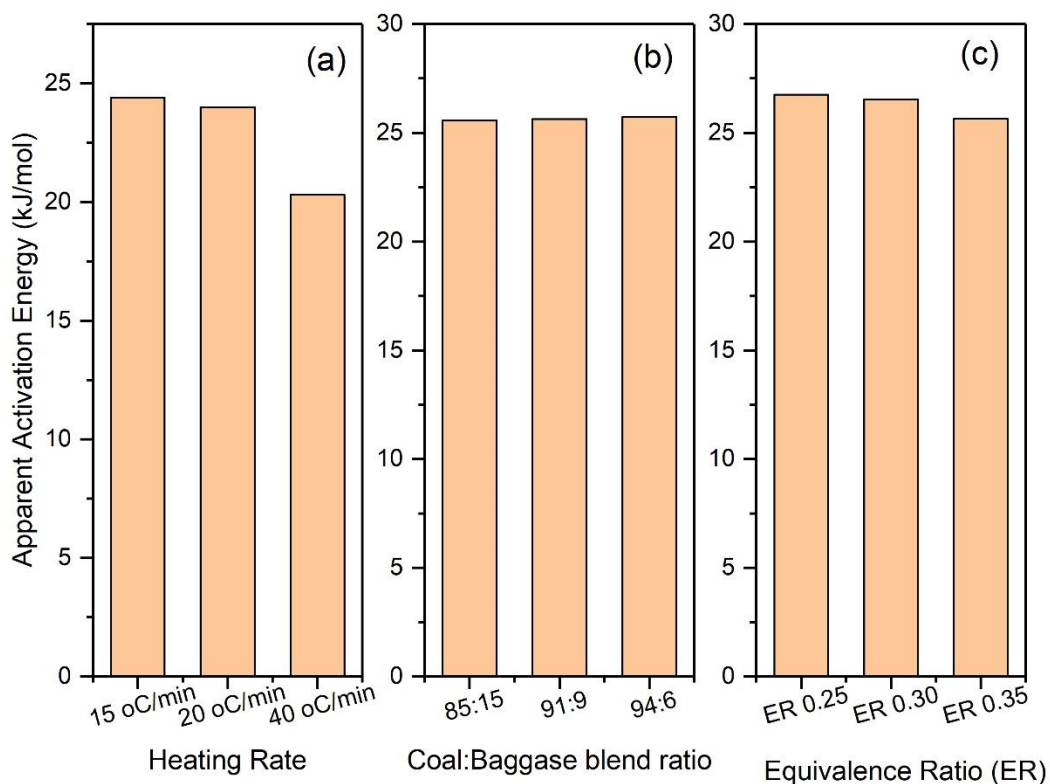
563

564 Figure 10. Apparent activation energies of the investigated raw fuels obtained from non-
565 isothermal thermogravimetric analysis: (a) biomass samples and (b) coal samples.

566 The effect of heating rate on activation energy is illustrated in **Figure 11**. The 91:9 coal–bagasse
567 blend at a heating rate of 20 °C min⁻¹ exhibited the most favorable overall kinetic response,
568 corresponding to the best conversion performance observed in Section 3.4. Although thermal
569 conversion can occur at lower and higher heating rates, the kinetic data indicate that the
570 intermediate heating rate provides a more favorable balance between heat supply and effective

571 progression of the reaction. This supports the earlier conclusion that $20\text{ }^{\circ}\text{C min}^{-1}$ is the most
572 appropriate heating rate among the tested values for the co-gasification of the selected blend.

573 The influence of feed composition on activation energy is presented in **Figure 11**. As the fraction
574 of bagasse in the blend increased, the activation energy generally decreased, reflecting the
575 increasing contribution of the more reactive biomass component. This trend is consistent with the
576 enhanced volatile content and oxygen availability associated with biomass addition. However,
577 although higher biomass addition improved reactivity, it also reduced the heating value of the
578 blend. Therefore, the most suitable feed composition was not simply the one with the lowest
579 activation energy, but rather the one that provided the best overall balance between reactivity and
580 fuel quality. On this basis, the 91:9 blend was identified as the most suitable composition for
581 further co-gasification analysis.



582

583 **Figure 11.** Effect of operating variables on the apparent activation energy of coal–bagasse

584 blends: (a) heating rate, (b) feed composition, and (c) equivalence ratio.

585 The effect of equivalence ratio on activation energy is shown in Figure 11. The activation energies

586 were 26.75, 26.54, and 25.64 kJ mol⁻¹ for the 91:9 blend at ER values of 0.25, 0.30, and 0.35,

587 respectively. Although the activation energy decreased slightly with increasing ER, the overall

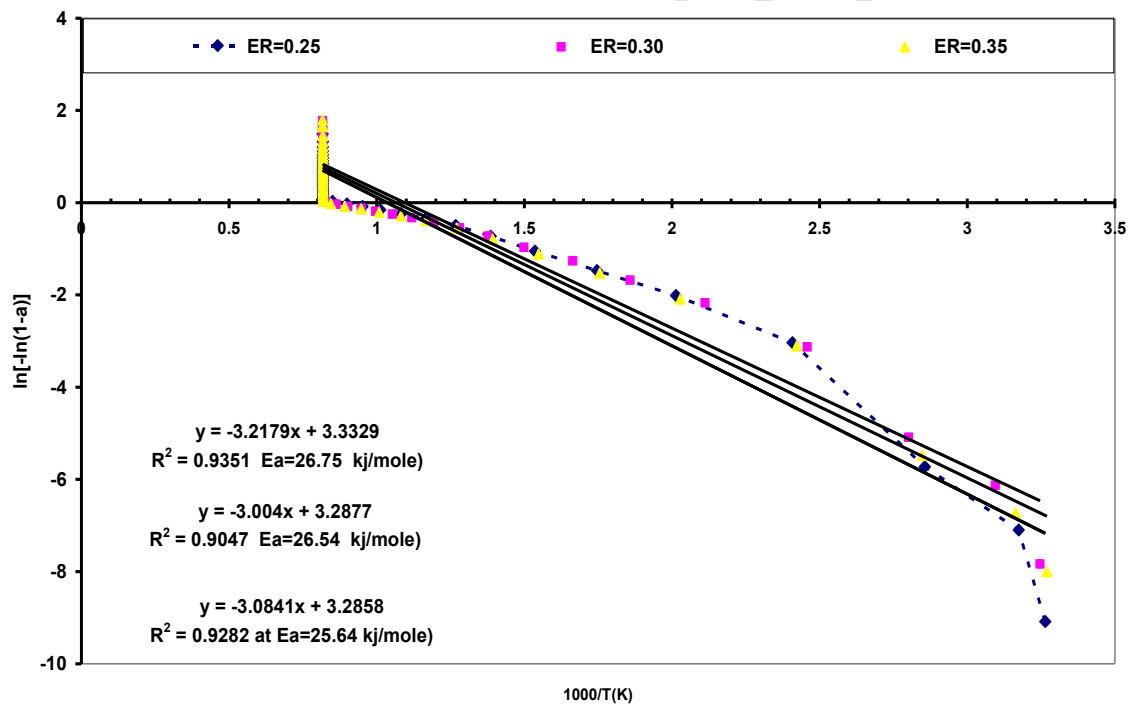
588 assessment of the process indicated that ER = 0.30 provided the most favorable condition when

589 conversion efficiency and operational suitability were considered together. This suggests that the

590 optimum ER should not be selected solely on the basis of minimum activation energy, but rather

591 on the combined interpretation of conversion behavior, thermal performance, and kinetics.

592 Overall, the kinetic analysis confirms the trends already observed in the physicochemical and
593 thermogravimetric results. Bagasse was identified as the most reactive biomass, Chamalang coal
594 as the most suitable coal, and the 91:9 coal–bagasse blend as the most favorable feed composition.
595 In addition, a heating rate of 20 °C min⁻¹ and an equivalence ratio of 0.30 were found to provide
596 the most suitable operating conditions for co-gasification under the present thermogravimetric
597 framework. Thus, the kinetic results not only support the selection of the blend and operating
598 parameters but also strengthen the overall interpretation of the thermal conversion behavior of the
599 investigated fuels.



600

601 **Figure 12.** Effect of equivalence ratio on the frequency factor of the 91:9 coal–bagasse blend
602 under air-assisted thermogravimetric conditions.

603

604 **3.6 Optimum blend and operating condition**

605 The selection of the optimum blend and operating condition was based on a combined
606 interpretation of physicochemical properties, thermogravimetric conversion behavior, and
607 apparent kinetic parameters, rather than on a single parameter alone. Among the investigated
608 compositions, the 91:9 coal–bagasse blend showed the most favorable overall balance. Increasing
609 the bagasse fraction enhanced the reactivity of the blend because of the higher volatile matter and
610 oxygen-rich nature of biomass. However, excessive biomass addition also reduced the calorific
611 value of the blended fuel. Therefore, the 91:9 blend was selected because it provided improved
612 conversion behavior while maintaining acceptable fuel quality and kinetic response.

613 The heating-rate analysis showed that $20\text{ }^{\circ}\text{C min}^{-1}$ was the most suitable heating rate among the
614 tested values. At this heating rate, the 91:9 blend exhibited higher overall conversion than the
615 blends tested at 15 and $40\text{ }^{\circ}\text{C min}^{-1}$. This indicates that an intermediate heating rate provided a
616 more effective balance between heat transfer, devolatilization, and subsequent char conversion. At
617 a lower heating rate, the conversion process progressed more slowly, whereas at a higher heating
618 rate, rapid heating may have increased thermal gradients and reduced the effective time available
619 for complete char conversion.

620 The equivalence-ratio results also require combined interpretation. For the 91:9 blend, the apparent
621 activation energies were 26.75, 26.54, and 25.64 kJ mol^{-1} at ER values of 0.25, 0.30, and 0.35,
622 respectively. Although $\text{ER} = 0.35$ showed the lowest apparent activation energy, this value alone
623 does not necessarily represent the most suitable gasification condition. Under air-assisted
624 conditions, increasing ER increases oxygen availability, which can promote mass loss and reduce
625 the apparent activation energy. However, excessive oxidant supply may also shift the process

626 toward partial combustion rather than controlled gasification. Therefore, ER = 0.30 was selected
627 as a balanced TGA-based operating condition because it provided favorable conversion and kinetic
628 behavior without relying on the highest oxidant input.

629 Thus, the optimum condition established in this study corresponds to the 91:9 coal–bagasse blend
630 operated at a heating rate of 20 °C min⁻¹ and an equivalence ratio of 0.30. This optimum should
631 be interpreted as a thermogravimetric optimum for apparent thermal conversion and kinetic
632 behavior under air-assisted conditions. It should not be considered a universal optimum for
633 industrial gasification performance because final validation requires gasification experiments
634 involving syngas composition, tar content, gas heating value, carbon conversion efficiency, and
635 emission analysis.

636 **4. Conclusions**

637 This study evaluated the co-gasification suitability of selected indigenous coal, biomass, and coal–
638 bagasse blends using physicochemical characterization, non-isothermal thermogravimetric
639 analysis, and kinetic assessment. The results showed clear differences in the thermal conversion
640 behavior of the investigated fuels, confirming that fuel properties such as volatile matter, fixed
641 carbon, ash content, oxygen content, and heating value strongly influence co-gasification
642 performance. Among the individual biomass samples, bagasse exhibited the most favorable
643 behavior because of its high volatile matter, low ash content, and comparatively strong thermal
644 reactivity. Among the coal samples, Chamalang coal was found to be the most suitable because of
645 its balanced fuel characteristics, relatively low ash content, and favorable conversion behavior.
646 These findings justified the selection of bagasse and Chamalang coal for blended-fuel preparation.

647 The prepared coal–bagasse blends showed that moderate biomass addition improved the reactive
648 characteristics of the parent coal without causing a severe loss in fuel quality. Among the tested
649 blend ratios, the 91:9 coal–bagasse blend provided the most favorable overall balance between
650 conversion performance and calorific value. The operating-condition analysis further
651 demonstrated that thermal conversion was strongly influenced by particle size, heating rate, feed
652 composition, and equivalence ratio. The best overall conversion performance was obtained at a
653 heating rate of $20\text{ }^{\circ}\text{C min}^{-1}$ and an equivalence ratio of 0.30.

654 The kinetic analysis supported the thermogravimetric findings and confirmed the suitability of the
655 selected blend and operating conditions. Bagasse showed the lowest activation energy among the
656 biomass samples, while Chamalang coal exhibited the most favorable kinetic behavior among the
657 investigated coals. For the blended fuels, the 91:9 composition showed the most suitable kinetic
658 response, and the combined interpretation of conversion and activation energy results identified
659 the 91:9 blend operated at $20\text{ }^{\circ}\text{C min}^{-1}$ and $\text{ER} = 0.30$ as the optimum condition within the
660 investigated range. Overall, the results demonstrate that partial substitution of Chamalang coal
661 with bagasse can improve the co-gasification performance of the feedstock and may provide a
662 practical basis for the development and optimization of coal–biomass thermochemical conversion
663 systems. The study offers useful guidance for fuel selection and operating-condition optimization
664 in future co-gasification applications involving indigenous coal and agricultural biomass
665 resources.

666 Although the present study demonstrates improved apparent conversion and kinetic behavior of
667 coal–bagasse blends, quantitative confirmation of synergistic or antagonistic interaction was
668 beyond the scope of the available dataset. Future studies should include matched individual-fuel

669 and blend conversion profiles under identical operating conditions to calculate synergy indices and
670 more clearly distinguish additive, synergistic, and antagonistic effects during co-gasification. The
671 present study was limited to air-assisted thermogravimetric conditions; therefore, future work
672 should investigate coal–bagasse blends under steam, oxygen-enriched air, and mixed gasifying
673 atmospheres to further evaluate their suitability for industrial gasification systems. Since the
674 present work was limited to thermogravimetric mass-loss and kinetic analysis, future studies
675 should evaluate the selected coal–bagasse blends in a lab-scale gasifier with gas-composition and
676 tar-analysis systems to determine syngas quality, tar formation, gas heating value, and overall
677 gasification efficiency.

678 In practical applications, industries using coal-based thermal systems, such as sugar mills, brick
679 kilns, cement plants, and small-scale gasification units, could consider partial substitution of coal
680 with bagasse at the 91:9 coal–bagasse ratio after pilot-scale validation. Such utilization would
681 provide a productive pathway for consuming sugarcane bagasse residues while reducing the
682 amount of coal required for thermal conversion processes.

683 **Declaration of Generative AI and AI-assisted technologies in the writing** 684 **process**

685 During the preparation of this manuscript, the authors used ChatGPT (OpenAI, GPT-4) to improve
686 language clarity, grammar, and readability. The tool was used only for linguistic refinement and
687 not for scientific content generation, data analysis, interpretation, or image creation. The authors
688 reviewed and edited all AI-assisted text and take full responsibility for the content of the
689 manuscript.

690 No generative AI or AI-assisted tools were used to create, modify, or enhance any figures or
691 graphical materials in this work.

692 **References**

693 Abedin, T., Pasupuleti, J., Paw, J.K.S., Tak, Y.C., Islam, M.R., Basher, M.K., Nur-E-Alam, M.,
694 2025. From waste to worth: advances in energy recovery technologies for solid waste
695 management. *Clean Technol. Environ. Policy* 27, 5963-5989. [https://doi.org/10.1007/s10098-](https://doi.org/10.1007/s10098-025-03204-x)
696 [025-03204-x](https://doi.org/10.1007/s10098-025-03204-x)

697 Adeoye, O.O., Silva Lora, E.E., Andrade, R.V., Pupo, L.P., Jaén, R.L., 2026. Review of
698 Entrained flow Co-gasification Technology of Biomass with Different Fuels. *Fuel* 404, 136420.
699 <https://doi.org/10.1016/j.fuel.2025.136420>

700 Ali, M., Shakaib, M., Zaidi, A.A., Javed, M.A., Khan, S.Z., Aly Hassan, A., 2025. Performance
701 and Environmental Sustainability of Fish Waste Biodiesel on Diesel Engines. *Sustainability*.
702 <https://doi.org/10.3390/su17125385>

703 Ansari, I., Zaidi, A.A., Memon, A.H., Hussain, A., Haleem, A.B., 2026. Valorization of Textile
704 Cotton Waste and Textile Sludge into High-Quality Torrefied Biofuel Pellets: Fuel
705 Characteristics and Optimization. *Energies*. <https://doi.org/10.3390/en19061401>

706 Awais, M., Omar, M.M., Munir, A., li, W., Ajmal, M., Hussain, S., Ahmad, S.A., Ali, A., 2022.
707 Co-gasification of different biomass feedstock in a pilot-scale (24 kWe) downdraft gasifier: An
708 experimental approach. *Energy* 238, 121821. <https://doi.org/10.1016/j.energy.2021.121821>

709 Bajwa, D.S., Peterson, T., Sharma, N., Shojaeiarani, J., Bajwa, S.G., 2018. A review of densified
710 solid biomass for energy production. *Renew. Sustain. Energy Rev.* 96, 296-305.
711 <https://doi.org/10.1016/j.rser.2018.07.040>

712 Balaram, V., Manikyamba, C., 2026. Coal and Coal Combustion Byproducts as Promising
713 Resources for the Extraction of Rare Earth Elements for the Current Energy Transition. *Geol. J.*
714 n/a. <https://doi.org/10.1002/gj.70210>

715 de Oliveira, T.R., Tannous, K., de Lima, E.C.T., 2022. Pyrolysis of the hybrid energy cane:
716 thermal decomposition and kinetic modeling using non-isothermal thermogravimetric analysis. *J.*
717 *Therm. Anal. Calorim.* 147, 7431-7448. <https://doi.org/10.1007/s10973-021-11028-2>

718 Fryda, L., Panopoulos, K., Vourliotis, P., Pavlidou, E., Kakaras, E., 2006. Experimental
719 investigation of fluidised bed co-combustion of meat and bone meal with coals and olive
720 bagasse. *Fuel* 85, 1685-1699. <https://doi.org/10.1016/j.fuel.2006.01.020>

721 Gong, J., Yang, L., 2024. A Review on Flaming Ignition of Solid Combustibles: Pyrolysis
722 Kinetics, Experimental Methods and Modelling. *Fire Technol.* 60, 893-990.
723 <https://doi.org/10.1007/s10694-022-01339-7>

724 Habib, M.I., 2026. Quantifying Solar Irradiation and Photovoltaic Energy Yield at Optimal Tilt
725 Angles: A Case Study of Gojra, Punjab, Pakistan. *J. Energy, Mater. Sustain.* 2, 18-38.
726 <https://doi.org/10.66173/jenmas.2026.18>

727 Inayat, A., Dafalla, M., Asaad, S., Jamil, F., Al-Haj, L., Shah, F.M., Ghenai, C., Shanableh, A.,
728 2025. Sustainable Energy Production From Waste: A Review of Hybrid Approaches Combining
729 Anaerobic Digestion and Gasification. *Int. J. Energy Res.* 2025, 6644084.
730 <https://doi.org/10.1155/er/6644084>

731 Jamil, R., Zaidi, A.A., Rai, R., Memon, A.H., Aijaz, A., Asif, M., 2026. Chapter 19 - Global
732 market potential and economic aspects of microalgae for biofuel production, in: Özkaya, B., Ali,
733 M., Zaidi, A.A., Naseer, M.N.B.T.-S.P. of M.B. as a B.F. (Eds.), Woodhead Series in Bioenergy.
734 Woodhead Publishing, pp. 535-561. <https://doi.org/10.1016/B978-0-443-29269-9.00013-7>

735 Koyunoğlu, C., Tolay, M., 2025. Co-gasification of Turkish lignite and three plastic wastes in a
736 lab-scale updraft gasifier: case-study equilibrium (gibbs free energy), openfoam CFD, analytical
737 validation, and experimental-range benchmarking. *Energy Convers. Manag.* X 28, 101372.
738 <https://doi.org/10.1016/j.ecmx.2025.101372>

739 Lei, S., Xing, B., Lv, B., Fang, J., Zeng, H., Zhang, C., Hou, Y., Wang, X., 2026. Advancements
740 in ultra-low ash coal: preparation techniques, applications, and future prospects for clean and
741 high-value utilization. *Int. J. Coal Prep. Util.* 46, 931-956.
742 <https://doi.org/10.1080/19392699.2025.2484316>

743 Luo, Z., Zhou, J., 2025. Thermal Conversion of Biomass BT - Handbook of Climate Change
744 Mitigation and Adaptation, in: Lackner, M., Sajjadi, B., Chen, W.-Y. (Eds.), . Springer Nature
745 Switzerland, Cham, pp. 1233-1289. https://doi.org/10.1007/978-3-031-84483-6_27

746 Mohlala, L.M., Bodunrin, M.O., Awosusi, A.A., Daramola, M.O., Cele, N.P., Olubambi, P.A.,
747 2016. Beneficiation of corncob and sugarcane bagasse for energy generation and materials
748 development in Nigeria and South Africa: A short overview. *Alexandria Eng. J.* 55, 3025-3036.
749 <https://doi.org/10.1016/j.aej.2016.05.014>

750 NREL, 1995. Alkali Deposits Found in Biomass Power Plants: A Preliminary Investigation of
751 Their Extent and Nature. Volume 1 [WWW Document]. URL
752 <https://digital.library.unt.edu/ark:/67531/metadc664004/> (accessed 4.25.24).

753 Nussipov, D., Akimbekov, N., Tastambek, K., Digel, I., Aimagambetov, A., Xiangrong, L.,
754 Yaya, W., Ackley, L., Zhailauova, G., 2026. Resource recovery from low-rank coal and
755 livestock manure for sustainable agroecosystems: a review. Arch. Microbiol. 208, 204.
756 <https://doi.org/10.1007/s00203-026-04758-0>

757 Preciado, J.E., Ortiz-Martinez, J.J., Gonzalez-Rivera, J.C., Sierra-Ramirez, R., Gordillo, G.,
758 2012. Simulation of Synthesis Gas Production from Steam Oxygen Gasification of Colombian
759 Coal Using Aspen Plus®. Energies. <https://doi.org/10.3390/en5124924>

760 Pribadi, G.A.D., Noble, A., 2026. Gasification of Indonesia's Low-Rank Coal: A Comparative
761 Review of Technology Options and Contextual Considerations. Fuel 414, 138280.
762 <https://doi.org/10.1016/j.fuel.2026.138280>

763 Puig-Arnavat, M., Bruno, J.C., Coronas, A., 2010. Review and analysis of biomass gasification
764 models. Renew. Sustain. Energy Rev. 14, 2841-2851. <https://doi.org/10.1016/j.rser.2010.07.030>

765 Quan, C., Ravelomanantsoa, V.S., Olazar, L., Santamaria, L., Lopez, G., Liu, L., Gao, N., 2026.
766 Thermochemical conversion of waste into energy: a review. Environ. Chem. Lett. 24, 295-320.
767 <https://doi.org/10.1007/s10311-025-01889-6>

768 Rodjeen, S., Mekasut, L., Kuchontara, P., Piumsomboon, P., 2006. Parametric studies on
769 catalytic pyrolysis of coal-biomass mixture in a circulating fluidized bed. Korean J. Chem. Eng.
770 23, 216-223. <https://doi.org/10.1007/BF02705719>

771 Rodrigues, R., Marcilio, N., Trierweiler, J., Godinho, M., 2011. Thermodynamic efficiency
772 analysis of gasification of high ash coal and biomass, in: International Conference on Coal
773 Science & Technology. Oviedo, Spain.

774 Sarwar, A., Nasiruddin Khan, M., Azhar, K.F., 2012. Kinetic studies of pyrolysis and
775 combustion of Thar coal by thermogravimetry and chemometric data analysis. J. Therm. Anal.
776 Calorim. 109, 97-103. <https://doi.org/10.1007/s10973-011-1725-0>

777 Senneca, O., Salatino, P., Chirone, R., 1999. A fast heating-rate thermogravimetric study of the
778 pyrolysis of scrap tyres. Fuel 78, 1575-1581. [https://doi.org/10.1016/S0016-2361\(99\)00087-3](https://doi.org/10.1016/S0016-2361(99)00087-3)

779 Si, F., Zhang, H., Feng, X., Xu, Y., Zhang, L., Zhao, L., Li, L., 2024. Thermodynamics and
780 synergistic effects on the co-combustion of coal and biomass blends. J. Therm. Anal. Calorim.
781 149, 7749-7761. <https://doi.org/10.1007/s10973-024-13310-5>

782 Tarani, E., Chrissafis, K., 2024. Isoconversional methods: A powerful tool for kinetic analysis
783 and the identification of experimental data quality. Thermochim. Acta 733, 179690.
784 <https://doi.org/10.1016/j.tca.2024.179690>

785 Tian, B., Wang, J., Qiao, Y., Huang, H., Xu, L., Tian, Y., 2023. Understanding the pyrolysis
786 synergy of biomass and coal blends based on volatile release, kinetics and char structure.
787 Biomass and Bioenergy 168, 106687. <https://doi.org/10.1016/j.biombioe.2022.106687>

788 TUMULURU, J.S., WRIGHT, C.T., 2010. A REVIEW ON BIOMASS DENSIFICATION
789 TECHNOLOGIE FOR ENERGY APPLICATION. United States.
790 <https://doi.org/10.2172/1016196>

791 Ungureanu, N., Vlăduț, N.-V., Biriș, S.-Ștefan, Ionescu, M., Gheorghiuță, N.-E., 2025. Municipal
792 Solid Waste Gasification: Technologies, Process Parameters, and Sustainable Valorization of
793 By-Products in a Circular Economy. Sustainability. <https://doi.org/10.3390/su17156704>

794 Vamvuka, D., Kakaras, E., Kastanaki, E., Grammelis, P., 2003. Pyrolysis characteristics and
795 kinetics of biomass residuals mixtures with lignite☆. *Fuel* 82, 1949-1960.
796 [https://doi.org/10.1016/S0016-2361\(03\)00153-4](https://doi.org/10.1016/S0016-2361(03)00153-4)

797 Wang, Haiyan, Liu, S., Wang, Haoqi, Chao, J., Li, T., Ellis, N., Duo, W., Bi, X., Smith, K.J.,
798 2025. Thermochemical conversion of biomass to fuels and chemicals: a review of catalysts,
799 catalyst stability, and reaction mechanisms. *Catal. Rev.* 67, 57-129.
800 <https://doi.org/10.1080/01614940.2023.2275093>

801 Wang, P., Hedges, S., Casleton, K., Guenther, C., 2012. Thermal Behavior of Coal and Biomass
802 Blends in Inert and Oxidizing Gaseous Environments. *Int. J. Clean Coal Energ.* 1, 35-42.
803 <https://doi.org/10.4236/ijcce.2012.13004>

804 Yadav, D., Saha, S., Sahu, G., Chavan, P.D., Datta, S., Chauhan, V., Kumari, N., 2023. A
805 comparative review on thermal behavior of feedstocks during gasification via thermogravimetric
806 analyzer. *J. Therm. Anal. Calorim.* 148, 329-354. <https://doi.org/10.1007/s10973-022-11757-y>

807 Yao, X., Liu, Q., Kang, Z., An, Z., Zhou, H., Xu, K., 2023. Quantitative study on thermal
808 conversion behaviours and gas emission properties of biomass in nitrogen and in CO₂/N₂
809 mixtures by TGA/DTG and a fixed-bed tube furnace. *Energy* 270, 126904.
810 <https://doi.org/10.1016/j.energy.2023.126904>

811 Youssef, M.A., Wahid, S.S., Mohamed, M.A., Askalany, A.A., 2009. Experimental study on
812 Egyptian biomass combustion in circulating fluidized bed. *Appl. Energy* 86, 2644-2650.
813 <https://doi.org/10.1016/j.apenergy.2009.04.021>

814 Zakaria, Z., Mohd Ishak, M.A., Abdullah, mohd fauzi, Ismail, K., 2010. Thermal Decomposition
815 Study of Coals, Rice Husk, Rice Husk Char and Their Blends During Pyrolysis and Combustion

816 via Thermogravimetric Analysis. Int. J. Chem. Technol. 2, 78-87.

817 <https://doi.org/10.3923/ijct.2010.78.87>

818 Zein, S.H., 2026. Thermodynamic Analysis of Plastic Waste Conversion to Hydrogen: Heat

819 Integration and System Performance-A Review. Thermo. <https://doi.org/10.3390/thermo6010014>

820 Zhang, Xuefei, Li, Y., Zhang, Xianwen, Ma, P., Xing, X., 2023. Co-combustion of municipal

821 solid waste and hydrochars under non-isothermal conditions: Thermal behaviors, gaseous

822 emissions and kinetic analyses by TGA-FTIR. Energy 265, 126373.

823 <https://doi.org/10.1016/j.energy.2022.126373>

ACCEPTED MANUSCRIPT